ROYAL SOCIETY OF CHEMISTRY

COMMUNICATION

Check for updates

Synthesis of a Co–Mo sulfide catalyst with a hollow structure for highly efficient hydrodesulfurization of dibenzothiophene†

Guangci Li, [iD] *[a] Li Yue,[b] Ruikun Fan,[a] Di Liu [iD][c] and Xuebing Li*[a]

A facile template-free method is developed to prepare porous Co–Mo sulfide sub-microtubes with open-ended structures *via* sulfurization of the Co–Mo precursor in an ethanol solution of CS_2. The hollow structure significantly improves the exposure degree of active components, resulting in an ultra-high activity for HDS of dibenzothiophene.

Hydrodesulfurization (HDS), particularly ultra-deep HDS, has become one of the most important hydrorefining processes for transportation fuels because of the increasingly stringent environmental regulations and air pollution issues worldwide.[1] Currently, supported transition metal sulfides, such as Co(Ni)Mo/γ-Al_2O_3 and Ni(Co)W/γ-Al_2O_3, are the most commonly used HDS catalysts; nevertheless, they are not able to reduce the sulfur content to an ultra-low level of the specifications under normal reaction conditions because of the limited loading amount of active components.[2] Recently, unsupported transition metal sulfides, containing at least two transition metals, have come into the picture because of their excellent HDS activity. Impressively, an unsupported trimetallic Ni–Mo–W catalyst called NEBULA has been reported, exhibiting at least three times higher HDS activity than supported CoMo/γ-Al_2O_3 and NiMo/γ-Al_2O_3 catalysts.[3] It is believed that the super high activity originating from abundant metal components can generate more catalytically active centers than the supported catalysts after a pre-sulfurization process. Unlike supported catalysts, however, active metals cannot be well dispersed on the unsupported catalyst surface

without any support, thus most of them which are within the catalyst particles have never been used and therefore wasted. For this reason, the atom efficiency and intrinsic activity of unsupported catalysts are still lower than those of supported catalysts,[4] which without a doubt limits their further application in industrial refinery. Based on this, numerous efforts thus have been made to develop effective methods for solving this problem,[5] wherein most of them are directed to increasing the surface area of unsupported catalysts by adding various additives during preparation. Although the specific activities of the catalysts were enhanced, the utilization of active metals has not been improved significantly. Therefore, finding efficient methods to improve the utilization of active metals within unsupported catalyst particles remains a challenging subject.

Nowadays, inorganic materials with hollow micro/nanostructures are of great interest due to their novel physicochemical properties.[6] Among these hollow structures, open-ended tube-like structures, which offer an open space inside the particles, are favorable for improving the exposure degree of inner atoms and their utilization. In view of this, preparing an unsupported HDS catalyst constructed from transition metal sulfide particles with tube-like structures is a promising approach to develop existing unsupported catalysts. Although various transition metal sulfide nanotubes have been synthesized, including MoS_2 and WS_2,[7] single MoS_2 or WS_2 without the promotion of Co and Ni atoms cannot achieve satisfactory HDS activities.[8] Thus, it would be desirable if a facile and effective method for the preparation of Co(Ni)-promoted Mo(W)S_2 with tube-like structures could be developed. However, relevant studies are rarely reported.

Herein, we prepared bimetallic Co–Mo sulfide sub-microtubes with open-ended structures through a facile sulfurization process of Co–Mo precursors under mild conditions. Because of the hollow structure inside the sub-microtubes, the resultant catalysts displayed excellent activity for HDS of dibenzothiophene (DBT), as compared to those

[a] Key Laboratory of Biofuels, Qingdao Institute of Bioenergy and Bioprocess Technology, Chinese Academy of Sciences, Qingdao 266101, P.R. China. E-mail: ligc@qibebt.ac.cn, lixb@qibebt.ac.cn
[b] Institute of Materials Science and Engineering, Ocean University of China, Qingdao 266110, P.R. China
[c] College of Chemical and Environmental Engineering, Shandong University of Science and Technology, Qingdao 266590, P.R. China
† Electronic supplementary information (ESI) available. See DOI: 10.1039/c7cy01724c

without hollow structures. The high catalytic activity is thought to be attributed to the abundant corner sites of surface MoS_2 slabs that are favorable for the desulfurization of DBT.

The Co–Mo precursor can be prepared through a co-precipitation process from $Co(CH_3COO)_2 \cdot 4H_2O$ and $(NH_4)_6Mo_7O_{24} \cdot 4H_2O$ in an ethanol–water mixed solution at 85 °C for 4 h. As shown in Fig. 1a and b, the obtained precursor is composed of one-dimensional rod-like particles with smooth surfaces. The uniform contrast of the particles in Fig. 1b indicates their solid and dense characteristics. The XRD pattern of the Co–Mo precursor (Fig. S1a in the ESI†) shows that most of the diffraction peaks can be well assigned to the standard patterns for the $CoMoO_6 \cdot 0.9H_2O$ phase (JCPDS No. 14-0086), and several weak diffraction peaks are attributed to the $CoMoO_4$ phase (JCPDS No. 15-0493).[9] The high-resolution TEM (HRTEM) image in Fig. 1b reveals well-resolved lattice planes of Co–Mo precursor particles, and the interplanar spacing measured (6.69 Å) is very close to that of the (001) planes of the $CoMoO_6 \cdot 0.9H_2O$ phase, indicating a preferential growth along the direction parallel to the (001) planes.

The sulfurization process of the Co–Mo precursor was carried out at 160 °C and 2.0 MPa H_2 for 6 h, using an ethanol solution of CS_2 as a sulfurization agent. The sharp contrast between the interior and the wall of the sub-microtubes suggests that the rod-like structures of the precursor have evolved into open-ended tube-like structures completely (Fig. 1c) after the sulfurization. Although the sizes of sub-microtubes are different, their wall thickness (ca. 10–20 nm) is relatively uniform. The corresponding XRD pattern reveals that the crystalline structure of the $CoMoO_4$ phase transformed into an amorphous structure (Fig. S1b†). Since the color of the Co–Mo precursor changes from violet to black after the sulfurization, the amorphous structure is considered to be Co–Mo polysulfide. After calcination at 400 °C for 4 h under a N_2 atmosphere, the polysulfides decomposed and re-leased their extra sulfur atoms, resulting in the appearance of the diffraction peaks of the MoS_2 (JCPDS No. 74-0932) and Co_9S_8 (JCPDS No. 86-2273) phases (Fig. S1c†). Despite the obvious change in crystalline structure of the sub-microtubes, their morphology and particle size remained nearly the same (Fig. 1d), which proved their good structural stability under high temperature treatment.

The structural evolution of the Co–Mo precursor during the sulfurization reaction was investigated to understand the formation process of the tube-like structure. The duration of the sulfurization varied from 0 to 3.0 h, where 0 h means that the reaction system was heated to 160 °C and then cooled down to room temperature immediately, and the evolution of morphology and crystalline structure against duration are shown in Fig. S2 and S3.† For comparison, another sulfurization reaction was conducted under the same conditions except that ethanol was replaced with decalin as solvent. After 6 h, the Co–Mo precursors were well transformed into sulfides (Fig. S4†), while the solid structures remained unchanged (Fig. S5†), indicating that the ethanol solvent plays a key role in the formation of tube-like structures.

In the presence of H_2, CS_2 can be easily converted into H_2S which then reacts with the Co–Mo precursors. In general, sulfurization starts from the external surface of the oxide precursor particles, and then proceeds inwards through the diffusion of sulfur atoms from the outer layer until the oxide precursor has been converted into sulfide completely;[10] the whole process needs several hours because the diffusion rate of sulfur atoms in the interior of the particles is very slow. Interestingly, this process can be finished within 1 h in this work, which reveals that ethanol really matters. Based on the above results, the possible formation process of the tube-like structure is schematically illustrated in Fig. 2. Initially, one proportion of the metal atoms on the surface of the particles is sulfurized, and the other is dissolved in ethanol to form metal ions at the same time. These metal ions are thought to be rapidly sulfurized into sulfides, and then deposited on the rod-like particle surface, which generate many small sulfide nanoparticles eventually during the dissolution–
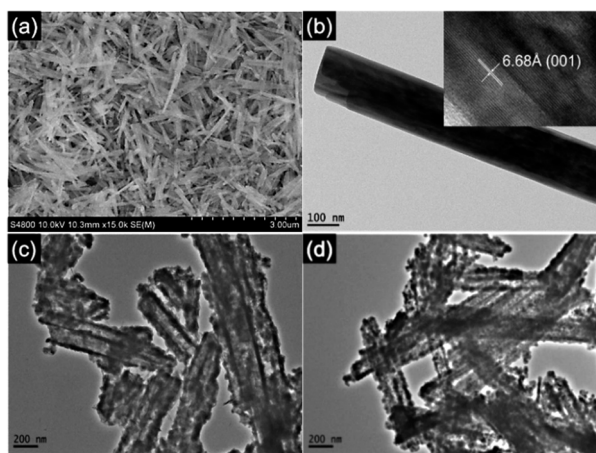

Fig. 1 SEM (a) and TEM (b–d) images of different samples: (a and b) Co–Mo precursor and HRTEM image (inset), (c) fresh Co–Mo sulfide sub-microtubes, and (d) calcined Co–Mo sulfide sub-microtubes.
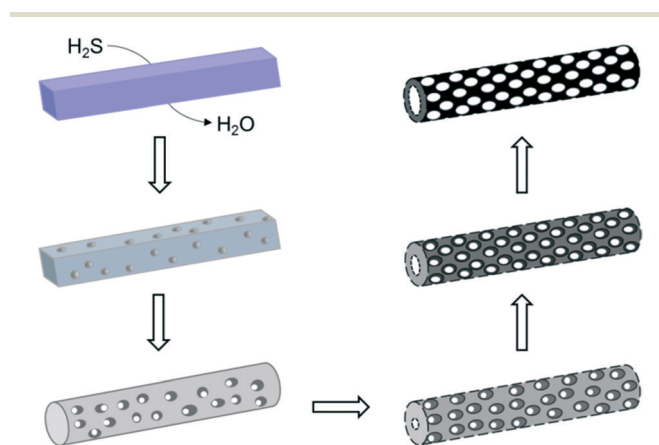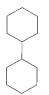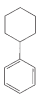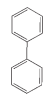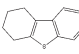

Fig. 2 Formation of the Co–Mo sulfide sub-microtubes from the Co–Mo precursor with rod-like structures.

Table 1 Conversion of DBT under different conditions

Catalyst	Temperature (°C)	Conversion[a] (%)	Product distribution (wt%)				Reaction rate[b] (mmol g_{cat}^{-1} h^{-1})
Co–Mo sub-microtubes	260	88.2	1.9	9.0	84.3	4.6	—
	280	94.6	2.2	12.2	81.3	4.3	—
	300	96.8	2.1	17.8	76.8	3.3	14.5
Co–Mo sub-microrods	300	32.8	—	6.8	89.2	3.0	1.78

[a] Reaction conditions: catalyst (0.2 g), DBT (0.8 g), decalin (39.2 g), initial H_2 pressure (2.0 MPa), stirring rate (600 rpm), reaction duration (4 h). [b] The reaction rate was calculated based on the kinetics experiments (Fig. S11).
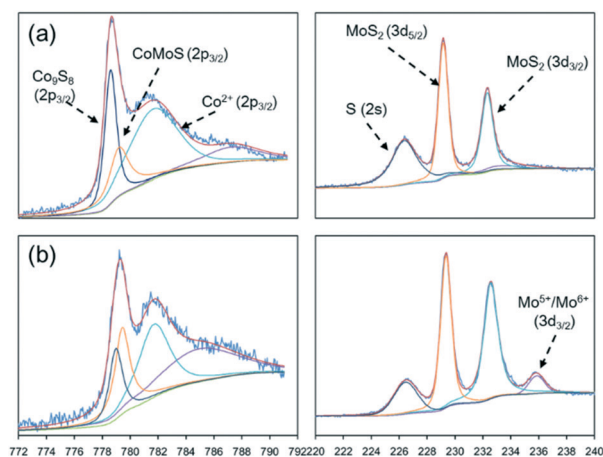
sulfurization–deposition process (Fig. S2b†). As the sulfurization continues, the dissolution–sulfurization–deposition process is repeated, which makes the formed sulfide nanoparticles grow gradually (Fig. S2d†). Because the metal sulfide is chemically passive, ethanol as an "etching agent" can only dissolve the inner unsulfurized metal atoms. Along with the dissolution, many separate voids are increasingly created inside the rod-like particles which then connected with one another, finally forming the integrated tube-like structure (Fig. S2f†). It is confirmed that the etching effect of ethanol accelerates the sulfurization of the inner metal atoms and encourages the formation of tube-like structures.

By means of an atomic absorption spectrometer, the ethanol solution after sulfurization is analyzed, and only 1.9 ppm Co and 53.3 ppm Mo are detected, showing that during the formation of the hollow structures, there is hardly any loss of active metals. To be more specific, the active metals etched in ethanol re-deposit onto the particle surface to construct the sub-microtubes. This synthetic method is surely helpful for preparing other bimetallic sulfides or oxides with tube-like structures.

The HDS activity of the as-prepared Co–Mo sulfide sub-microtubes was investigated in a continuously stirred tank reactor at 2.0 MPa H_2 for a certain duration, using a decalin solution of DBT as the model reactant. For comparison, as a reference catalyst, a Co–Mo sulfide sample without a hollow structure was synthesized through a conventional method (see the ESI†). Because the above used Co–Mo precursor is the same as that for the preparation of the sub-microtube catalyst, the effect of particle size on the catalytic activity can be ignored here. The TEM image shows that the reference catalyst is composed of solid rod-like particles that inherit the structure of the Co–Mo precursor (Fig. S6†). The XRD pattern shows that its crystalline structure is very similar to that of the sub-microtube catalyst (Fig. S7†); however, its HDS activities are much more different. As shown in Table 1, the reaction rate of DBT over the sub-microtube catalyst was calculated to be 14.5 mmol g_{cat}^{-1} h^{-1}, about 8.2 times as much as that over the reference catalyst, which could be attributed to the difference in microstructure. As measured using N_2 sorption isotherms (Fig. S8a†), the reference catalyst's specific surface area (SSA) is 17.1 m^2 g^{-1}, and the pore size is mostly below 5 nm (Fig. S8b†), while the sub-microtube catalyst's SSA reaches 49.4 m^2 g^{-1}, and the number of mesopores larger than 5 nm increases markedly. Because the inner diameter of most sub-microtubes is around 100 nm which cannot be measured by the N_2 sorption method, the increment of the SSA is thought to be dependent on the increased mesopores, which mainly originated from the gaps between the particles that construct the sub-microtube walls, and the gaps are obtained from the ethanol etching process.

Commonly, higher surface areas and more mesopores can supply more active sites, and thus the two catalysts are characterized by the H_2-TPR technique in order to confirm this view (Fig. S9†). Apparently, the TPR profiles of the two catalysts show a strong reduction peak at 150–350 °C, assigned to the reduction of surface sulfur atoms that are weakly bonded to Mo atoms.[11] It is agreed that if the surface sulfur atoms are reduced, the coordinatively unsaturated sites (CUS) will be created *in situ*, which are responsible for the HDS activity.[12] And in this work, according to the reduction peak areas, the hydrogen consumption for the sub-microtube catalyst is calculated to be about twice as much as that of the reference catalyst, thus more CUS will be created on the surface of the sub-microtube catalyst during the reaction in the presence of H_2, which will surely lead to a higher HDS activity.

Fig. 3 XPS spectra of Co–Mo sulfide catalysts with different microstructures: (a) sub-microrod and (b) sub-microtube.

This journal is © The Royal Society of Chemistry 2017

Catal. Sci. Technol., 2017, **7**, 5505–5509 | **5507**

Moreover, considering that the CUS may originate from a separate MoS_2 phase or MoS_2 phase decorated by Co atoms (so-called Co–Mo–S phase), to further understand the nature of the CUS, XPS characterization was thus carried out (Fig. 3). The results show that for the two catalysts only a small amount of CUS is generated from the Co–Mo–S phase, in which the number of CUS from the Co–Mo–S phase for the sub-microtube catalyst (32.2%) is more than that for the sub-microrod catalyst (20.7%) (Table S1†). Considering that XPS only detects the near-surface of materials, and the testing depth of XPS is generally less than 10 nm which is smaller than the thickness of the sub-microtube wall, thus the internal surface of the sub-microtubes cannot be detected, which means that the actual content of the Co–Mo–S phase would be higher. In addition, the peak of Co 2p assigned to the Co oxide state is observed, which may be because the surface Co of the fresh catalyst is easily oxidized after exposure to air during sample transfer.[13] For Mo-based HDS catalysts, although some controversial views about the nature of the active sites still exist,[14] it is widely accepted that CUS located on the edge of the MoS_2 slabs are the active sites for HDS reactions. However, the length and stacking number of the MoS_2 slabs can affect the location and distribution of CUS, thus catalysts with the same number of CUS may vary in HDS activities. In view of this, these two catalysts are analyzed by HRTEM (Fig. S10†), and the characteristics of the morphology of (Co)MoS_2 slabs were statistically evaluated (see Table S3†). The results show that the (Co)MoS_2 slabs on the reference catalyst particles look like several long and straight lines, while those on the sub-microtube catalyst particles are much shorter and more curved, which by contrast supply more corner sites that are responsible for improving the direct desulfurization capabilities of DBT.[15] As a result, the sub-microtube catalyst reveals a much higher HDS activity than the reference catalyst, although the proportion of the Co–Mo–S phase for the sub-microtube catalyst is 1.5 times higher compared to that of the reference catalyst.

Generally, the HDS process of DBT undergoes two parallel routes: direct desulfurization (DDS) and hydrodesulfurization (HYD). The DDS route leads to the formation of biphenyl compounds through direct C–S bond rupture, while the HYD route, *via* a hydrogenation–desulfurization process, leads to the formation of cyclohexylbenzene. As shown in Tables 1 and S4,† the predominant liquid product is biphenyl for the two catalysts. It is reported that the main effect of cobalt promotion on MoS_2 is electronic by nature,[16] which strongly enhances the DDS route.[17] Therefore, the conversion of DBT in this work mainly undergoes the DDS route.

In order to compare with published results, the HDS activity of the Co–Mo sub-microtube catalyst was described in different expressions, such as the apparent reaction rate (mol g_{cat}^{-1} s^{-1} or mol mol_{metal}^{-1} s^{-1}), rate constant (L g_{cat}^{-1} s^{-1}), and TOF value (s^{-1}). As shown in Table S2,† the catalyst prepared in this work demonstrates a much higher activity for HDS of DBT than unsupported Co–Mo and Ni–Mo catalysts.

Note that the involved reaction temperature and H_2 pressure are lower than those of published works, which means that under the same reaction conditions, the as-prepared catalyst will exhibit a higher activity.

To sum up, in order to sufficiently use the active components of an unsupported catalyst, a facile method involving co-precipitation and low-temperature sulfurization in ethanol solution is developed to prepare porous Co–Mo sulfide sub-microtubes with open-ended structures. The formation of sub-microtubes is closely dependent on the dissolving and etching functions of ethanol. This special structure supplies a relatively high SSA and active component exposure degree, which generate more HDS active sites, resulting in better HDS performance.

Conflicts of interest

There are no conflicts to declare.

Acknowledgements

Notes and references

1 (*a*) K. G. Knudsen, B. H. Cooper and H. Topsøe, *Appl. Catal., A*, 1999, **189**, 205; (*b*) I. V. Babich and J. A. Moulijn, *Fuel*, 2003, **82**, 607.

2 (*a*) C. Song and X. Ma, *Appl. Catal., B*, 2003, **41**, 207; (*b*) C. Song, *Catal. Today*, 2003, **86**, 211.

3 (*a*) S. L. Soled, S. Miseo, R. Krycak, H. Vroman, T. C. Ho and K. Riley, *US Pat.*, 6299760, 2000; (*b*) S. L. Soled, S. Miseo and Z. Hou, *US Pat.*, 7544632, 2005.

4 (*a*) D. Genuit, P. Afanasiev and M. Vrinat, *J. Catal.*, 2005, **235**, 302; (*b*) L. Wang, Y. Zhang, Y. Zhang, Z. Jiang and C. Li, *Chem. – Eur. J.*, 2009, **15**, 12571.

5 (*a*) H. Nava, F. Pedraza and G. Alonsoa, *Catal. Lett.*, 2005, **99**, 65; (*b*) B. Yoosuk, J. H. Kim, C. Song, C. Ngamcharussrivichai and P. Prasassarakich, *Catal. Today*, 2008, **130**, 14; (*c*) C. Yin, L. Zhao, Z. Bai, H. Liu, Y. Liu and C. Liu, *Fuel*, 2013, **107**, 873.

6 (*a*) Y. Zhu, J. Shi, W. Shen, X. Dong, J. Feng, M. Ruan and Y. Li, *Angew. Chem., Int. Ed.*, 2005, **44**, 5083; (*b*) J. Liu, S. Qiao, J. Chen, X. Lou, X. Xing and G. Lu, *Chem. Commun.*, 2011, **47**, 12578; (*c*) B. Xia, H. Wu, X. Wang and X. Lou, *J. Am. Chem. Soc.*, 2012, **134**, 13934; (*d*) L. Yu, H. Wu and X. Lou, *Adv. Mater.*, 2013, **25**, 2296.

7 (*a*) R. Tenne, L. Margulis, M. Genut and G. Hodes, *Nature*, 1992, **360**, 444; (*b*) C. M. Zelenski and P. Dorhout, *J. Am. Chem. Soc.*, 1998, **120**, 734; (*c*) J. Chen, N. Kuriyama, H. Yuan, H. T. Takeshita and T. Sakai, *J. Am. Chem. Soc.*,

2001, **123**, 11813; (*d*) J. Chen, S.-L. Li, Q. Xu and K. Tanaka, *Chem. Commun.*, 2002, 1722.

8 (*a*) B. S. Clausen, H. Topsøe and F. E. Massoth, in *Catalysis – Science and Technology*, ed. J. R. Anderson and M. Boudart, Springer, New York, 1996, vol. 11; (*b*) D. D. Whitehurst, T. Isoda and I. Mochida, *Adv. Catal.*, 1998, **42**, 345.

9 (*a*) K. Eda, Y. Uno, N. Nagai, N. Sotani and M. S. Whittinghan, *J. Solid State Chem.*, 2005, **178**, 2791; (*b*) M. Liu, L. Kong, C. Lu, X. Li, Y. Luo and L. Kang, *Mater. Lett.*, 2013, **94**, 197.

10 (*a*) Y. Yin, R. M. Rioux, C. K. Erdonmez, S. Hughs, G. A. Somorjai and A. P. Alivisatos, *Science*, 2004, **304**, 711; (*b*) H. Cao, X. Qian, C. Wang, X. D. Ma, J. Yin and Z. Zhu, *J. Am. Chem. Soc.*, 2005, **127**, 16024.

11 P. Afanasiev, *Appl. Catal., A*, 2006, **303**, 110.

12 H. Topsøe, *Appl. Catal., A*, 2007, **322**, 3.

13 (*a*) J. Gao, C. Jia, J. Li, F. Gu, G. Xu, Z. Zhong and F. Su, *Ind. Eng. Chem. Res.*, 2012, **51**, 10345; (*b*) Q. Liu, F. Gu, X. Liu, Y. Liu, H. Li and Z. Zhong, *Appl. Catal., A*, 2014, **488**, 37.

14 (*a*) F. Bataille, J. Lemberton, P. Michaud, G. Pérot, M. Vrinat, M. Lemaire, E. Schulz, M. Breysse and S. Kasztelan, *J. Catal.*, 2000, **191**, 409; (*b*) P. A. Nikulshin, V. A. Salnikov, A. V. Mozhaev, P. P. Minaev, V. M. Kogan and A. A. Pimerzin, *J. Catal.*, 2014, **309**, 386.

15 A. K. Tuxen, H. G. Füchtbauer, B. Temel, B. Hinnemann, H. Topsøe, K. G. Knudsen, F. Besenbacher and J. V. Lauritsen, *J. Catal.*, 2012, **295**, 146–154.

16 (*a*) S. Harris and R. R. Chianelli, *J. Catal.*, 1986, **98**, 17–31; (*b*) R. R. Chianelli, G. Berhault, P. Raybaud, S. Kasztelan, J. Hafner and H. Toulhoat, *Appl. Catal., A*, 2002, **227**, 83–96.

17 (*a*) T. Kabe, A. Ishihara and Q. Zhang, *Appl. Catal., A*, 1993, **97**, L1–L9; (*b*) P. Michaud, J. L. Lemberton and G. Pérot, *Appl. Catal., A*, 1998, **169**, 343–353.